

## Experimental investigation of the suppressed superconducting gap and double-resonance mode in $\text{Ba}_{1-x}\text{K}_x\text{Fe}_2\text{As}_2$

S. Ideta<sup>1,2</sup>, N. Murai,<sup>3</sup> M. Nakajima,<sup>4</sup> R. Kajimoto<sup>3</sup>, and K. Tanaka<sup>1,2</sup>

<sup>1</sup>National Institutes of Natural Science, Institute for Molecular Science, Okazaki 444-8585, Japan

<sup>2</sup>The Graduate University for Advanced Studies (SOKENDAI), Okazaki 444-8585, Japan

<sup>3</sup>Materials and Life Science Division, J-PARC Center, Japan Atomic Energy Agency, Tokai, Ibaraki 319-1195, Japan

<sup>4</sup>Department of Physics, Graduate School of Science, Osaka University, Toyonaka 560-0043, Japan



(Received 5 February 2019; revised manuscript received 10 November 2019; published 23 December 2019)

$\text{Ba}_{1-x}\text{K}_x\text{Fe}_2\text{As}_2$  has an exotic physical property, i.e., the  $C_2$  spin-density-wave phase suddenly changes to the  $C_4$  magnetic phase, and superconductivity is suppressed within a narrow composition range around  $x = 0.25$ . We have investigated the doping dependence of the electronic structure of  $\text{Ba}_{1-x}\text{K}_x\text{Fe}_2\text{As}_2$  using angle-resolved photoemission spectroscopy (ARPES), and we found an anomaly in the superconducting (SC) gap structure only for  $x = 0.25$  in both the hole and electron Fermi surfaces. We also propose that the mechanism of a newly observed double-resonance peak by inelastic neutron scattering is understandable because of the SC gap obtained by ARPES. Our discovery reveals the important relationship between the  $C_4$ -magnetic phase and superconductivity, and it provides an opportunity to survey the underlying relationship between the SC gap and the resonance mode in the hole-doped iron-based superconductor.

DOI: [10.1103/PhysRevB.100.235135](https://doi.org/10.1103/PhysRevB.100.235135)

### I. INTRODUCTION

An interplay between the intertwined electron (charge, orbital, spin) and lattice degrees of freedom is a crucial issue to elucidate the physical properties in condensed-matter physics. A fundamental question is to what extent these degrees of freedom contribute to superconductivity. Iron-based superconductors (Fe-SCs) are an ideal material to investigate the role of the degrees of freedom in an unconventional superconducting (SC) mechanism. Nematicity of Fe-SC, which is defined as the breaking of rotational symmetry, is one of the unresolved issues for the relationship with superconductivity in the underdoped regime [1–4]. In hole-doped  $\text{BaFe}_2\text{As}_2$  (Ba122) systems, thermal expansion, specific heat, and neutron diffraction measurements of  $(\text{Ba,Sr,Ca})\text{Fe}_2\text{As}_2$  doped with Na/K have revealed the magnetic order without breaking the  $C_4$  symmetry in the underdoped regime, the  $C_4$ -magnetic phase (MP), which is interpreted as the double- $\mathbf{Q}$  magnetic order in the absence of orbital ordering associated with the electronic nematicity [5–7]. Furthermore, these materials show that the SC transition temperature ( $T_c$ ) is suppressed by  $\sim 15$ – $50\%$  [6–10], which is similar to the cuprate at  $1/8$  doping [11,12]. Although these intriguing physical properties are universally observed in the hole-doped Ba122 system, the microscopic mechanism driven by the intertwined degrees of freedom and the  $T_c$  suppression remains unclear.

In this work, we report a combined study performed by angle-resolved photoemission spectroscopy (ARPES) and inelastic neutron scattering (INS) on  $\text{Ba}_{1-x}\text{K}_x\text{Fe}_2\text{As}_2$  (BK) ( $x = 0.25$ ) to elucidate the mechanism of superconductivity and its suppression. As a comparison, we also measured two other doping levels above and below  $x = 0.25$ . The present ARPES study reveals that the SC gap on hole Fermi surfaces (FSs) shows isotropic nodeless gaps, which are

strongly suppressed for  $x = 0.25$ . Additionally, a significant  $k_z$  dependence of the SC gap is discovered on an electron FS. This implies that the SC gap anisotropy would assist in the construction of the intriguing double-resonance peak in INS.

### II. EXPERIMENTS

High-quality single crystals of  $\text{Ba}_{1-x}\text{K}_x\text{Fe}_2\text{As}_2$  [ $x = 0.21$ (BK21),  $T_c \sim 18$  K;  $x = 0.25$ (BK25),  $T_c \sim 26$  K;  $x = 0.3$ (BK30),  $T_c \sim 36$  K] were grown by the self-flux technique.  $T_c$  is defined as the point of zero resistance and individually characterized by electronic resistivity measurement in all samples. The  $C_4$ -MP was present in all BK25 samples, which we confirmed by electronic resistivity measurement [13]. ARPES experiments were carried out at BL 7U of UVSOR-III Synchrotron. Clean sample surfaces were obtained by cleaving single crystals *in situ* in an ultrahigh vacuum better than  $6 \times 10^{-9}$  Pa. Total energy resolution was set at  $\sim 6$  meV. Measured samples in the present study were obtained from the same batch of INS. INS experiments were performed by using the 4SEASONS time-of-flight spectrometer at Japan Proton Accelerator Research Complex (J-PARC). The INS data presented in the present study were collected at  $T = 5$  and 30 K using incident neutron energies ( $E_i$ ) of 13.5 and 36.8 meV. During the data collection, the sample was held at a fixed angle with the  $c$ -axis parallel to the incident neutron beam [13].

### III. EXPERIMENTAL RESULTS

The neutron scattering cross section is proportional to the dynamical spin susceptibility,  $\chi''(\mathbf{q},\omega)$ , whose momentum and energy dependence depends strongly on the details of the electron band dispersion. Therefore, neutron scattering can

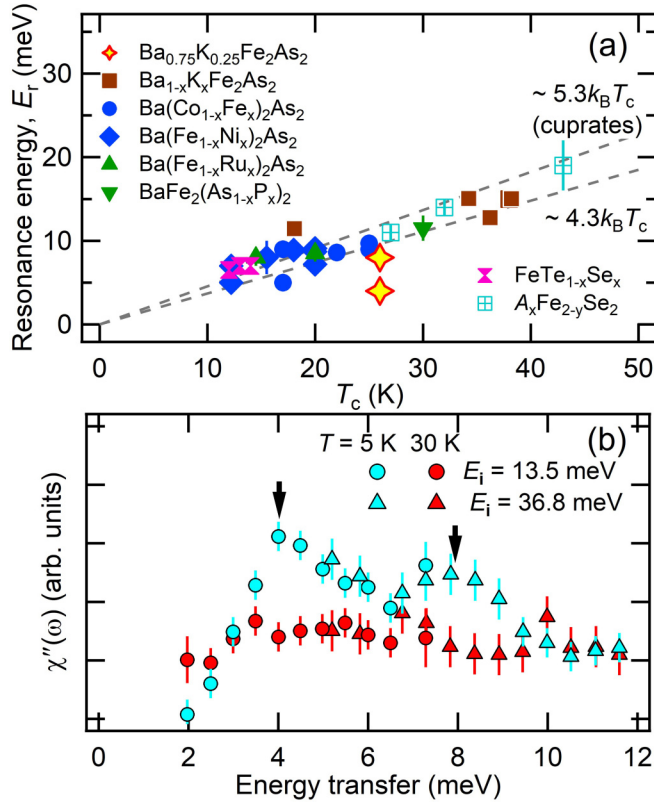


FIG. 1. Resonance peak energy observed by inelastic neutron scattering. (a) The data are extracted from Refs. [14–32]. Stars indicate the result of BK25. (b) Double-resonance peak in BK25 obtained by INS. The arrows correspond to the energies shown in (a).

be a sensitive probe of the underlying electronic structure. In particular, the SC gap manifests itself as a pronounced peak in  $\chi''(\mathbf{q}, \omega)$ . The appearance of the peak in the SC state, which is called neutron spin resonance, depends on the relative signs of the SC gap on different portions of the FS separated by momentum  $\mathbf{q}$ , and thus provides insight into the SC gap structure. The resonance energy obtained by INS is proportional to  $T_c$  ( $E_r \sim 4.3\text{--}5.3k_B T_c$ ) for several Fe-SCs and cuprates, as shown in Fig. 1(a) [14–32]. In the present study, INS experiments provided an intriguing result on BK25, which showed the  $C_4$ -MP; the double-resonance peak is observed as shown in Figs. 1(b) and 4(n). Although the double-resonance peak has been reported in previous INS studies, for example in electron-doped  $\text{NaFe}_{1-x}\text{Co}_x\text{As}$  [14], the double-resonance peak in the hole-doped BaK25 shown in the present study is a new experimental finding. In Fig. 1(a), while  $E_{r1} \sim 8$  meV falls on the straight dotted line, which represents the form of  $E_r \sim 4.3k_B T_c$ ,  $E_{r2} \sim 4$  meV deviates from the line by  $\sim 50\%$ . This experimental evidence suggests that there is a SC gap anomaly corresponding to the  $T_c$  suppression in BK25. Considering the strong sensitivity of the spin excitations to the underlying electronic structure, one can expect the modulation of the SC gap in BK25, which can be explored in a more detailed and quantitative manner by using ARPES.

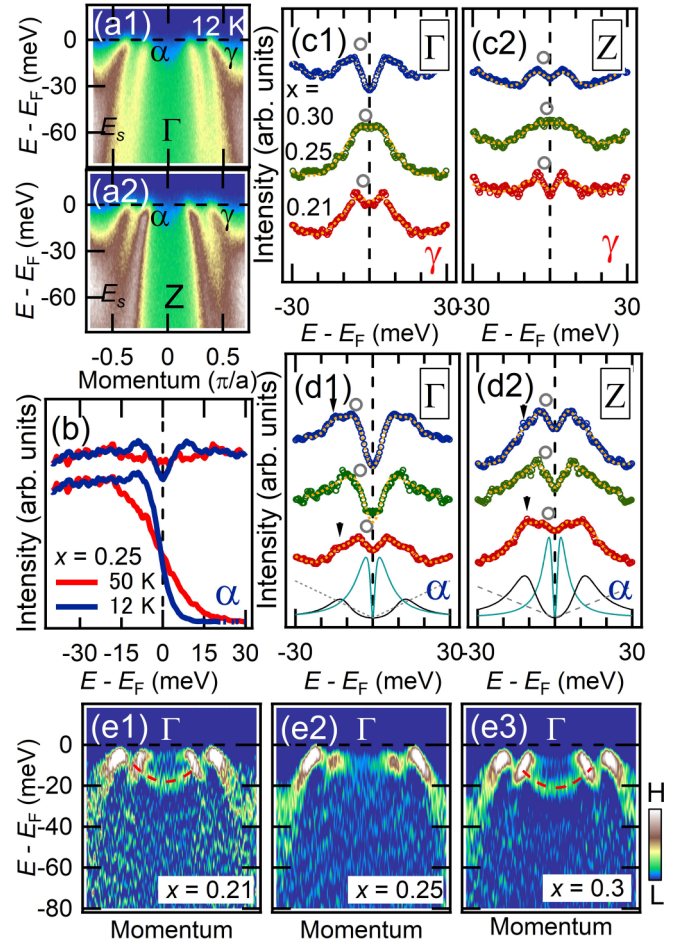


FIG. 2. SC-gap distribution on the hole FSs of  $\text{Ba}_{1-x}\text{K}_x\text{Fe}_2\text{As}_2$ . (a1),(a2) Photoemission intensities near the BZ center with 21 ( $\Gamma$ ) and 32 eV ( $Z$ ) photons. (b) Temperature dependence of ARPES spectra of  $k_F$  at  $\Gamma$ . (c1),(c2) Symmetrized EDCs of  $\gamma$  at  $k_F$  for  $x = 0.21, 0.25$ , and  $0.3$  samples. (d1),(d2) The same as in (c1) and (c2) of  $\alpha$ . The gray circles in (c1)–(d2) are guides to the eyes for the SC gap, which is determined by fitting with the common phenomenological SC spectral function as illustrated in (d1) and (d2) [51]. Results are shown in the  $x = 0.21$  sample as an example. (e1)–(e3) Second derivative photoemission intensity with respect to energy along  $\Gamma$ -X. Arrows in panels (d1) and (d2) show the peak structure arising from the overlapped electronlike parabolic band.

Figures 2(a1) and 2(a2) show the ARPES intensity plot as a function of energy and momentum, which corresponds to  $\Gamma$  and  $Z$ , respectively. We observed at least two-hole bands for  $\Gamma$  using  $s$  polarization, which indicates that the degenerate  $d_{yz}/d_{xz}$  bands (inner hole FS) and the  $d_{x^2-y^2}$  band (outer hole FS) were present at  $\Gamma$  [13,33,34]. Hereafter, the hole bands at the Brillouin zone (BZ) center are designated as  $\alpha$ ,  $\beta$ , and  $\gamma$  for the inner, middle, and outer hole FSs, respectively. However, the  $\gamma$  band, corresponding to the  $d_{xy}$  band at the high-symmetry line on  $Z$ , and one of the middle bands,  $d_{xz}(\beta)$ , were not clearly observed using  $s$  polarization due to different orbital symmetry [13,34,35]. To confirm the electronic structure of BK25 in the  $k_z$  direction, we performed FS mapping along the  $k_z$  direction [13], which was similar to the previous ARPES study [35].

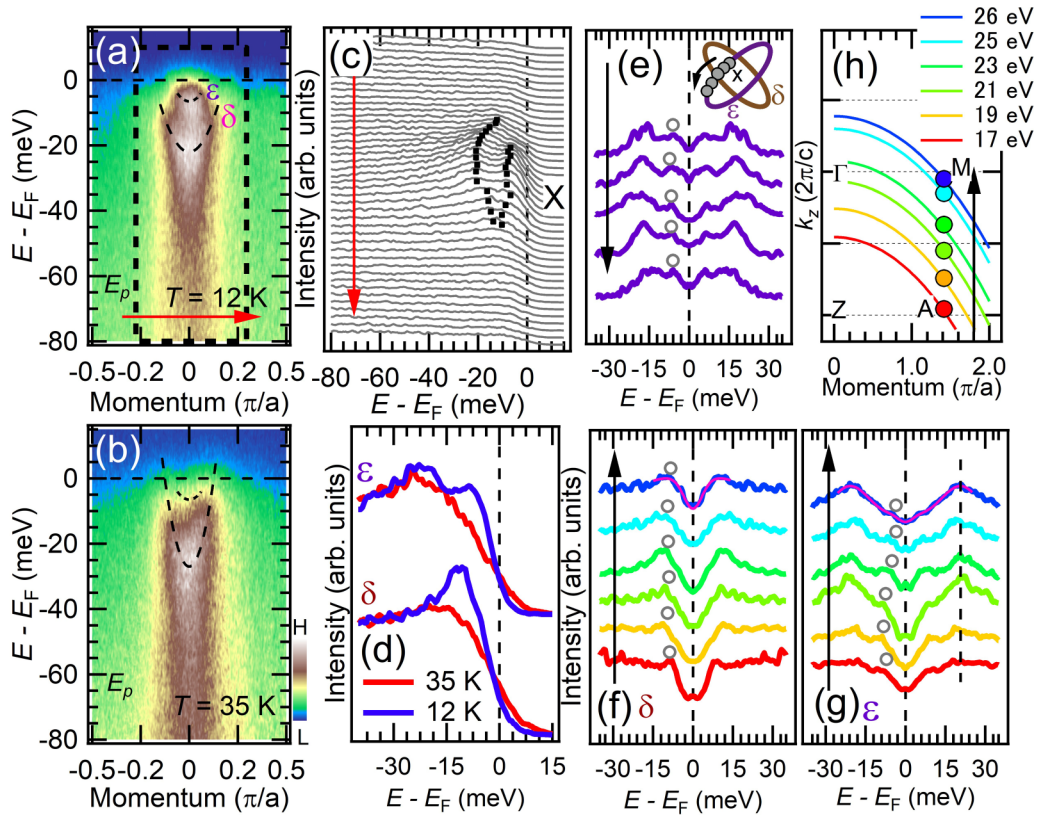


FIG. 3. SC-gap distribution on the electron FSs of BK25. (a),(b) Photoemission intensities at the BZ corner taken at 23 eV photons below and above  $T_c$ , respectively. (c) Raw spectra in (a) enclosed by the dotted line. (d) Temperature dependence of ARPES spectra for  $\varepsilon$  and  $\delta$  at  $k_F$  taken at 23 eV photons. (e) Symmetrized raw spectra at  $k_F$  on the  $\varepsilon$  band taken at 23 eV photons. (f),(g)  $k_z$  dependence of the symmetrized spectra measured on the  $\delta$  and  $\varepsilon$  bands. (h) Measured  $k_z$ 's are taken at 17–26 eV photons, which corresponds to the  $k_z$  of  $A(Z)$ - $M(\Gamma)$ . The gray circles in the spectra are guides to the eyes for the SC gaps determined by fitting as shown by a pink curve in (f) and (g) [51] in order to exclude the effect of mixing for the  $\varepsilon$  and  $\delta$  bands.

To elucidate the character of the SC gap on the hole FSs, Fig. 2(b) shows the temperature dependence of the ARPES spectrum near  $E_F$  measured across  $T_c$  at the Fermi momentum ( $k_F$ ) for the  $\alpha$  band. The energy-distribution curve (EDC) shows a SC peak in the SC state while this disappears in the normal state. To eliminate the effect of the Fermi-Dirac (FD) distribution function, we symmetrized the ARPES spectra measured above and below  $T_c$ . On decreasing the temperature, the spectral weight near  $E_F$  is transferred to the higher binding energy below  $T_c$ , and the symmetrized EDC shows a peak at  $\sim 7$ – $8$  meV, which suggests the opening of a SC gap. Symmetrized EDCs obtained for BK21, BK25, and BK30 at the  $k_F$ 's of the  $\alpha$  and  $\gamma$  bands are shown in Figs. 2(c1)–2(d2) for comparison. While the SC peak ( $x = 0.21, 0.3$ ) is far from the  $E_F$ , which indicates that the SC gap is observed on the  $\alpha$  and  $\gamma$  FSs, we found that the SC peak of BK25 moves toward  $E_F$ , which indicates the decrease or almost closure of SC gaps for the  $\gamma$  band.

In Figs. 2(e1)–2(e3), the second-derivative ARPES intensity plots measured at the BZ center are presented. The folding of the electron bands to  $\Gamma$  was observed below the spin-density-wave transition temperature [36] in the wide doping regime from the underdoping to overdoping [37]. Although the ARPES intensity plots of BK ( $x = 0.21, 0.3$ ) show a strong band folding of the electronlike band, which is reflected by

a finite shoulder or peak structure in EDC [a black arrow in Figs. 2(d1) and 2(d2)] denoted by a red dotted curve, the reconstructed electronic structure is washed out in BK25. This indicates that the spectral weight of a reconstructed band structure is small. This was proposed to arise from the recently reported antiferroelectric instability [37] being suppressed around  $x = 0.25$  and/or the fact that the  $C_4$ -MP fluctuation may affect the electronic structure, which indicates that the SC gap on the  $\gamma$  FS of BK25 would be influenced by the  $C_4$ -MP.

Figure 3 provides the detailed SC gap distribution of the electron bands designated as  $\varepsilon$  and  $\delta$  for two electron FSs at the BZ corner ( $X$ ). ARPES intensity plots below and above  $T_c$  at  $X$  are shown in Figs. 3(a) and 3(b), respectively. As shown in Fig. 3(a), small and large parabolic electron bands, which are indicated by dotted curves, are present in the SC state. A detailed dispersive feature is shown by EDC [Fig. 3(c)], which was extracted from the enclosed area of Fig. 3(a). A sharp peak was observed near the  $E_F$ , and the SC gap is more clearly seen in Fig. 3(d). To precisely determine the SC gap size and its momentum dependence, we performed an ARPES study at several  $k_F$  and  $k_z$  points for the  $\varepsilon$  and  $\delta$  bands. The EDCs of the  $\varepsilon$  band obtained after symmetrization are shown in Fig. 3(e) and exhibited the presence of an isotropic SC gap ( $\Delta_\varepsilon \sim 6.5$  meV). For the  $\delta$  band, the electron pocket was

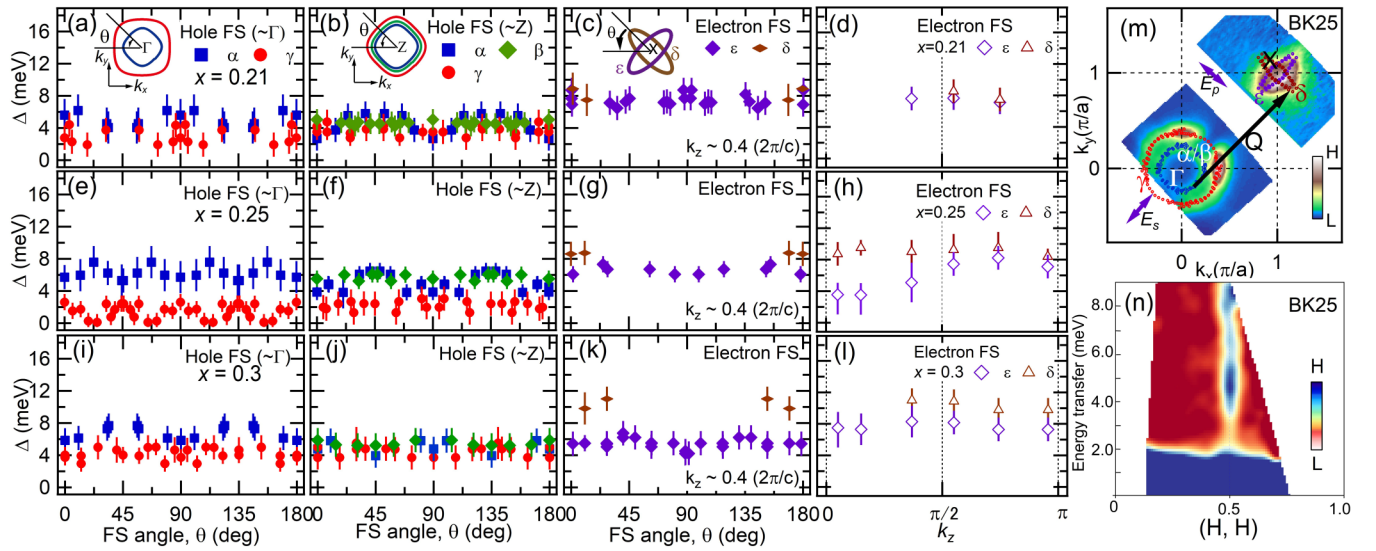


FIG. 4. Momentum and doping dependences of the SC gap. (a),(b) SC gaps (BK21) on the  $k_x$ - $k_y$  plane for hole FSs at  $\Gamma$  and Z plotted as functions of FS angle,  $\theta$ . (c) SC gaps (BK21) on the  $k_x$ - $k_y$  plane for the electron FSs as functions of FS angle,  $\theta$ . (e)–(g) The same sets of (a)–(c), respectively, but for BK25. (i)–(k) The same sets of (a)–(c), respectively, but for BK30. The SC gap values in the  $k_x$ - $k_y$  plane are plotted by assuming a symmetry. (d),(h),(l)  $k_z$  dependence of the SC gaps at the BZ corner from  $\Gamma$  ( $k_z = 0$ ) to Z ( $k_z = \pi$ ). All SC gap values were determined by fitting [13,51]. (m) FS mapping around  $\Gamma$  and X.  $k_F$ 's are plotted by markers for each FS. (n) INS data observed at 5 K [13]. Two resonance modes are clearly observed at the energy transfers of  $\sim 8$  and  $\sim 4$  meV.

observed only near the BZ corner, and the SC gap values were similar to those in the previous studies ( $\Delta_\delta \sim 8.5$  meV) [38–40].

For the  $k_z$  direction, while the SC gap for the  $\delta$  band shows an isotropic gap [Fig. 3(f)], the EDC peak position, which reflects the SC gap for the  $\varepsilon$  band, does not seem to be constant [Fig. 3(g)], as shown by the gray circle decreases in going from A to M. This indicates that an anisotropic SC gap was observed along the  $k_z$  direction for the  $\varepsilon$  FS. Here, we need to pay attention to the fact that the mixing of the  $\varepsilon$  and  $\delta$  bands has an effect on the SC gap of the  $\varepsilon$  band. When the relative intensity changes between these two bands, the SC gap estimated from a peak position also changes. To overcome this effect, symmetrized EDCs were fitted by using the two phenomenological SC spectral functions [51]. Therefore, the distortion of the measured SC gap is considered to be small. In addition, note that in contrast with the previous ARPES study [36], the flat electron band in the SC state was not observed in this study. However, the SC gap of the  $\delta$  band almost corresponds to the energy of the flat band.

The doping and momentum dependence of the SC gap distribution on the hole and electron FSs is summarized as a function of FS angle ( $\theta$ ) and  $k_z$  momentum space (A–M) in Fig. 4. These SC gap values were determined by fitting with the common phenomenological function including the energy resolution [13,41]. The SC gap of the  $\gamma$  hole FS is strongly suppressed and shows a small value and/or almost zero on the entire FS ( $\Delta_\gamma \sim 0$ –2 meV) in BK25 [Figs. 4(e) and 4(f)], while the SC gap for BK21 and BK30 showed  $\Delta_\gamma \sim 3$  and 5 meV, respectively. The SC gap on the  $\alpha$  and  $\beta$  hole FSs shows an almost isotropic distribution ( $\Delta_{\alpha,\beta} \sim 4$ –6 meV), but moderately anisotropic for the  $\alpha$  FS in BK25. Here, the assignment of the inner band ( $\beta$ ) in the present study is different from the previous study [35] since in the recent

ARPES study it was concluded that the strongly enhanced SC gap of the  $\beta$  band ( $\Delta \sim 12$  meV) in Ref. [35] is a consequence of the folded electron band at X [37]. As for the SC gaps on the electron FS, the gaps for the  $\varepsilon$  FS have a nearly isotropic distribution, which is similar to the previous ARPES results [38–40,42]. However, we clearly observe that the SC gap on the  $\varepsilon$  FS depends on  $k_z$  momentum space, as shown in Fig. 4(h) (the  $\delta$  band shows an isotropic SC gap in the  $k_z$  direction), in contrast with the previous ARPES study for optimally doped samples [35]. The infinitesimal SC gap observed by the present ARPES study on BK25 corresponds to the results obtained by the heat capacity measurement [9], which is in contrast with the previous ARPES study [38]. The discrepancy possibly originates from whether the  $C_4$ -MP is actually present or not, which can be confirmed by the anomaly in the electronic resistivity. Here we confirmed that the  $C_4$ -MP was indeed present in the present study [13] in contrast to the previous study even if the difference in hole concentration is small.

Now we move on to a comparison of the present ARPES study with the INS results. As shown in Fig. 4(n), spin excitations appear at  $\mathbf{Q} = (0.5, 0.5)$ , which corresponds to the nesting between the hole and electron FSs [43]. An important question concerns the origin of the double-resonance modes, which are separated in energy. Since  $\mathbf{Q}$  connects the FSs with different signs of the SC gaps, the resonance peak is formed at an energy of  $\omega \sim \Delta_h + \Delta_e$ , where  $\Delta_h$  and  $\Delta_e$  are the SC gap at the hole and electron FSs, respectively. This is a reasonable approximation when the SC gap size is comparable for all hole FSs ( $\Delta_{h,\alpha/\beta} \sim \Delta_{h,\gamma}$ ). However, when the energy difference of the SC gap is sufficiently large within the hole FSs ( $\Delta_{h,\alpha/\beta} \neq \Delta_{h,\gamma}$ ), one can expect two distinct resonances at energies of  $\omega \sim \Delta_{h,\alpha/\beta} + \Delta_e$  and  $\omega \sim \Delta_{h,\gamma} + \Delta_e$  [18]. This situation agrees qualitatively with the case of BK25, in which

the unequal SC gap at different bands gives rise to multiple spin resonance modes. On the other hand, there are some differences with Ref. [18]. As shown in Fig. 4(m), although the area of the  $\gamma$  FS ( $d_{x^2-y^2}$ ,  $d_{xy}$ ) is larger than that of the  $\varepsilon/\delta$  FS ( $d_{yz}/d_{yz}$ ,  $d_{x^2-y^2}$ ), the  $\alpha/\beta$  FS ( $d_{xz}/d_{yz}$ ) seems to be almost the same as the  $\varepsilon/\delta$  FS. The mismatch of the  $\gamma$ -FS and  $\varepsilon/\delta$ -FS area should lead to an incommensurability of the lower-energy resonance peak as reported in previous studies [18], which was not observed within the experimental  $\mathbf{Q}$  resolution [see Fig. 4(n)]. Another possible explanation for the origin of the double resonances is the  $k_z$  dependence of the SC gap on the  $\varepsilon$  FSs. Considering the good nesting condition between the  $\alpha/\beta$  and  $\varepsilon/\delta$  FSs, the presence of the orbital-dependent SC gaps within the electron FSs may produce the multiple resonance modes at  $\mathbf{Q} = (0.5, 0.5)$  [14,44]. In both cases, the origin of the double-resonance mode in BK25 is traced back to the presence of the  $C_4$ -MP that suppresses the SC gaps in a band-dependent manner. A reasonable and distinguishable theory, which could interpret the double-resonance mode derived from the different SC gap on the in-plane FS and/or the  $k_z$  dependent SC gap, is not yet available. To further evaluate the validity of the present finding, it is highly desirable to construct a theoretical investigation that would shed light on the relationship between the spin fluctuation spectrum and the underlying electronic structure of Fe-SCs.

#### IV. DISCUSSION

Comparing the electronic structure of the three doping levels, a key question in understanding the SC mechanism is why the  $\gamma$  SC gap is strongly suppressed only in BK25. The present study indicates that the suppressed SC gap of BK25 is likely to provide direct evidence corresponding to the  $T_c$  suppression. According to the previous ARPES study, the SC gap size on the hole FSs was almost identical in optimally doped  $\text{Ba}_{1-x}\text{K}_x\text{Fe}_2\text{As}_2$ , which was interpreted by the  $s_{++}$ -wave gap symmetry arising from orbital fluctuations [45]. Although the SC gaps on both the  $\alpha$  and  $\beta$  FSs of BK25 were almost identical, that on the  $\gamma$  FS is not explained by the orbital fluctuation. Therefore, the spin fluctuation due to the FS nesting between the  $\alpha/\beta$  ( $d_{yz}$ ,  $d_{xz}$ ) hole and  $\delta/\varepsilon$  ( $d_{yz}/d_{xz}$ ,  $d_{x^2-y^2}$ ) electron FSs [33,34] controls the pairing mechanism dominantly in K-Ba122 ( $x = 0.25$ ). A possible interpretation of the reduced SC gap leading to the  $T_c$  suppression in BK25 is the mismatch of the FS size between the outer hole and electron FSs.

Another interesting issue is that the  $T_c$  suppression in BK25 is smaller than that of  $\text{Ba}_{0.75}\text{Na}_{0.25}\text{Fe}_2\text{As}_2$  (BN25). A plausible interpretation is the existence of a competing electronic order. In the present study, the checkerboard-type electronic order, as observed in [46], was not found at the BZ corner. In fact, thermodynamic methods and infrared spectroscopy have

reported the existence of an itinerant double- $\mathbf{Q}$  magnetic order and checkerboard-like electronic structure in BK25 [47,48]. This may be because the electronic order is weak in BK25, where the charge order (CO) strongly couples with the spin order and competes with superconductivity [11,12]. This is consistent with a small- $T_c$  suppression of BK25 [9] compared with that of BN25 [8]. In  $\text{NbSe}_2$ , which shows both CO and superconductivity, photoemission, transport, and x-ray scattering measurements have indicated that the long-range CO does indeed compete with superconductivity, but the short-range CO assists it [49]. This indicates the strong interplay between the CO and superconductivity. In addition, the FS dependence of the SC gap has been observed in  $\text{NbSe}_2$  [41]. In analogy with dichalcogenides, the short-range CO is present in the  $C_4$ -MP to assist superconductivity in BK25. Compared with the ionic radius of barium ( $\text{Ba}^{2+}$ ), the difference in the ionic radius between sodium ( $\text{Na}^+$ ) and barium ( $\text{Ba}^{2+}$ ) is larger than that of potassium ( $\text{K}^+$ ), and therefore sodium substitution may cause a stronger chemical pressure than potassium. Therefore, the  $T_c$  suppression in BK25 might be small since the long-range CO is more stable for sodium substitution than for potassium. How the out-of-plane disorder affects the electronic structure of the FeAs layer is not yet clear in the Fe-SCs. However, it is plausible that the disorder effectively contributes to the microscopic SC mechanism as in cuprates [50].

#### V. SUMMARY

In conclusion, we have reported the high-resolution ARPES study on  $\text{Ba}_{1-x}\text{K}_x\text{Fe}_2\text{As}_2$ . We revealed in- and out-of-plane SC gaps on the hole and electron FSs. We successfully observed that the SC gap on the outer hole FS was suppressed, and we observed the  $k_z$  dependence of the SC gap on the  $\varepsilon$  FS. The SC gap anisotropy in the present ARPES study was compared with the double-resonance modes in INS. The electron band folding probably associated with high- $T_c$  superconductivity at the BZ center disappears in only the  $x = 0.25$  sample. These findings directly suggest the  $T_c$  suppression in the  $C_4$ -MP. Our present discoveries impose a strong constraint on the theoretical models to describe the universal SC mechanism of hole-doped Fe-SCs invoking the  $C_4$ -MP.

#### ACKNOWLEDGMENTS

We thank T. Shimojima and S. Ishida for inspiring discussion, and M. Sakai for experimental support at UVSOR. ARPES experiments were carried out at UVSOR-III Synchrotron (Proposals No. 28-529 and No. 28-549). This work was supported by Grant-in-Aid for Young Scientists (B) (15K17709) and Grant-in-Aid for Early-Career Scientists (18K13500), JSPS, Japan. Neutron scattering experiments at the Materials and Life Science Experimental Facility of J-PARC were carried out under Proposal No. 2015I0001.

- [1] R. M. Fernandes, A. V. Chubukov, and J. Schmalian, *Nat. Phys.* **10**, 97 (2014).
- [2] R. M. Fernandes and A. J. Millis, *Phys. Rev. Lett.* **111**, 127001 (2013).
- [3] T. Shimojima, Y. Suzuki, T. Sonobe, A. Nakamura, M. Sakano, J. Omachi, K. Yoshioka, M. Kuwata-Gonokami, K. Ono,

H. Kumigashira, A. E. Böhmer, F. Hardy, T. Wolf, C. Meingast, H. v. Löhneysen, H. Ikeda, and K. Ishizaka, *Phys. Rev. B* **90**, 121111(R) (2014).

- [4] Y. Ming, D. Lu, J.-H. Chu, J. G. Analytis, A. P. Sorini, A. F. Kemper, B. Moritz, S.-K. Mo, R. G. Moore, M. Hashimoto, W.-S. Lee, Z. Hussain, T. P. Devereaux, I. R.

- Fisher, and Z.-X. Shen, *Proc. Natl. Acad. Sci. (USA)* **108**, 6878 (2011).
- [5] D. D. Khalyavin, S. W. Lovesey, P. Manuel, F. Krüger, S. Rosenkranz, J. M. Allred, O. Chmaissem, and R. Osborn, *Phys. Rev. B* **90**, 174511 (2014).
- [6] J. M. Allred, S. Avci, D. Y. Chung, H. Claus, D. D. Khalyavin, P. Manuel, K. M. Taddei, M. G. Kanatzidis, S. Rosenkranz, R. Osborn, and O. Chmaissem, *Phys. Rev. B* **92**, 094515 (2015).
- [7] J. M. Allred, K. M. Taddei, D. E. Bugaris, M. J. Krogstad, S. H. Lapidus, D. Y. Chung, H. Claus, M. G. Kanatzidis, D. E. Brown, J. Kang, R. M. Fernandes, I. Eremin, S. Rosenkranz, O. Chmaissem, and R. Osborn, *Nat. Phys.* **12**, 493 (2016).
- [8] L. Wang, F. Hardy, A. E. Böhmer, T. Wolf, P. Schweiss, and C. Meingast, *Phys. Rev. B* **93**, 014514 (2016).
- [9] A. E. Böhmer, F. Hardy, L. Wang, T. Wolf, P. Schweiss, and C. Meingast, *Nat. Commun.* **6**, 7911 (2015).
- [10] A. Avci, O. Chmaissem, J. M. Allred, S. Rosenkranz, I. Eremin, A. V. Chubukov, D. E. Bugaris, D. Y. Chung, M. G. Kanatzidis, J.-P. Castellan, J. A. Schlueter, H. Claus, D. D. Khalyavin, P. Manuel, A. Daoud-Aladine, and R. Osborn, *Nat. Commun.* **5**, 3845 (2014).
- [11] A. J. Achkar, F. He, R. Sutarto, C. McMahan, M. Zwiebler, M. Hücker, G. D. Gu, R. Liang, D. A. Bonn, W. N. Hardy, J. Geck, and D. G. Hawthorn, *Nat. Mater.* **15**, 616 (2016).
- [12] B. Keimer, S. A. Kivelson, M. R. Norman, S. Uchida, and J. Zaanen, *Nature (London)* **518**, 179 (2015).
- [13] See Supplemental Material at <http://link.aps.org/supplemental/10.1103/PhysRevB.100.235135> for details of the present study.
- [14] C. Zhang, R. Yu, Y. Su, Y. Song, M. Wang, G. Tan, T. Egami, J. A. Fernandez-Baca, E. Faulhaber, Q. Si, and P. Dai, *Phys. Rev. Lett.* **111**, 207002 (2013).
- [15] G. Yu, Y. Li, E. M. Motoyama, and M. Greven, *Nat. Phys.* **5**, 873 (2009).
- [16] C. Zhang, M. Wang, H. Luo, M. Wang, M. Liu, J. Zhao, D. L. Abernathy, T. A. Maier, K. Marty, M. D. Lumsden, S. Chi, S. Chang, J. A. Rodriguez-Rivera, J. W. Lynn, T. Xiang, J. Hu, and P. Dai, *Sci. Rep.* **1**, 115 (2011).
- [17] J.-P. Castellan, S. Rosenkranz, E. A. Goremychkin, D. Y. Chung, I. S. Todorov, M. G. Kanatzidis, I. Eremin, J. Knolle, A. V. Chubukov, S. Maiti, M. R. Norman, F. Weber, H. Claus, T. Guidi, R. I. Bewley, and R. Osborn, *Phys. Rev. Lett.* **107**, 177003 (2011).
- [18] T. Das and A. V. Balatsky, *Phys. Rev. Lett.* **106**, 157004 (2011).
- [19] D. K. Pratt, A. Kreyssig, S. Nandi, N. Ni, A. Thaler, M. D. Lumsden, W. Tian, J. L. Zarestky, S. L. Bud'ko, P. C. Canfield, A. I. Goldman, and R. J. McQueeney, *Phys. Rev. B* **81**, 140510(R) (2010).
- [20] D. S. Inosov, J. T. Park, P. Bourges, D. L. Sun, Y. Sidis, A. Schneidewind, K. Hradil, D. Haug, C. T. Lin, B. Keimer, and V. Hinkov, *Nat. Phys.* **6**, 178 (2010).
- [21] M. D. Lumsden, A. D. Christianson, D. Parshall, M. B. Stone, S. E. Nagler, G. J. MacDougall, H. A. Mook, K. Lokshin, T. Egami, D. L. Abernathy, E. A. Goremychkin, R. Osborn, M. A. McGuire, A. S. Sefat, R. Jin, B. C. Sales, and D. Mandrus, *Phys. Rev. Lett.* **102**, 107005 (2009).
- [22] J. T. Park, D. S. Inosov, A. Yaresko, S. Graser, D. L. Sun, Ph. Bourges, Y. Sidis, Y. Li, J.-H. Kim, D. Haug, A. Ivanov, K. Hradil, A. Schneidewind, P. Link, E. Faulhaber, I. Glavatsky, C. T. Lin, B. Keimer, and V. Hinkov, *Phys. Rev. B* **82**, 134503 (2010).
- [23] M. Wang, H. Luo, J. Zhao, C. Zhang, M. Wang, K. Marty, S. Chi, J. W. Lynn, A. Schneidewind, S. Li, and P. Dai, *Phys. Rev. B* **81**, 174524 (2010).
- [24] S. Chi, A. Schneidewind, J. Zhao, L. W. Harriger, L. Li, Y. Luo, G. Cao, Z. Xu, M. Loewenhaupt, J. Hu, and P. Dai, *Phys. Rev. Lett.* **102**, 107006 (2009).
- [25] S. Li, Y. Chen, S. Chang, J. W. Lynn, L. Li, Y. Luo, G. Cao, Z. Xu, and P. Dai, *Phys. Rev. B* **79**, 174527 (2009).
- [26] J. Zhao, C. R. Rotundu, K. Marty, M. Matsuda, Y. Zhao, C. Setty, E. Bourret-Courchesne, J. Hu, and R. J. Birgeneau, *Phys. Rev. Lett.* **110**, 147003 (2013).
- [27] M. Ishikado, Y. Nagai, K. Kodama, R. Kajimoto, M. Nakamura, Y. Inamura, S. Wakimoto, H. Nakamura, M. Machida, K. Suzuki, H. Usui, K. Kuroki, A. Iyo, H. Eisaki, M. Arai, and S. I. Shamoto, *Phys. Rev. B* **84**, 144517 (2011).
- [28] A. D. Christianson, M. D. Lumsden, K. Marty, C. H. Wang, S. Calder, D. L. Abernathy, M. B. Stone, H. A. Mook, M. A. McGuire, A. S. Sefat, B. C. Sales, D. Mandrus, and E. A. Goremychkin, *Phys. Rev. B* **87**, 224410 (2013).
- [29] A. E. Taylor, R. A. Ewings, T. G. Perring, J. S. White, P. Babkevich, A. Krzton-Maziopa, E. Pomjakushina, K. Conder, and A. T. Boothroyd, *Phys. Rev. B* **86**, 094528 (2012).
- [30] A. E. Taylor, S. J. Sedlmaier, S. J. Cassidy, E. A. Goremychkin, R. A. Ewings, T. G. Perring, S. J. Clarke, and A. T. Boothroyd, *Phys. Rev. B* **87**, 220508(R) (2013).
- [31] G. Friemel, J. T. Park, T. A. Maier, V. Tsurkan, Y. Li, J. Deisenhofer, H.-A. Krug von Nidda, A. Loidl, A. Ivanov, B. Keimer, and D. S. Inosov, *Phys. Rev. B* **85**, 140511(R) (2012).
- [32] G. Friemel, W. P. Liu, E. A. Goremychkin, Y. Liu, J. T. Park, O. Sobolev, C. T. Lin, B. Keimer, and D. S. Inosov, *Europhys. Lett.* **99**, 67004 (2012).
- [33] Y. Zhang, F. Chen, C. He, B. Zhou, B. P. Xie, C. Fang, W. F. Tsai, X. H. Chen, H. Hayashi, J. Jiang, H. Iwasawa, K. Shimada, H. Namatame, M. Taniguchi, J. P. Hu, and D. L. Feng, *Phys. Rev. B* **83**, 054510 (2011).
- [34] W. Malaeb, T. Shimojima, Y. Ishida, K. Okazaki, Y. Ota, K. Ohgushi, K. Kihou, T. Saito, C. H. Lee, S. Ishida, M. Nakajima, S. Uchida, H. Fukazawa, Y. Kohori, A. Iyo, H. Eisaki, C.-T. Chen, S. Watanabe, H. Ikeda, and S. Shin, *Phys. Rev. B* **86**, 165117 (2012).
- [35] Y. Zhang, L. X. Yang, F. Chen, B. Zhou, X. F. Wang, X. H. Chen, M. Arita, K. Shimada, H. Namatame, M. Taniguchi, J. P. Hu, B. P. Xie, and D. L. Feng, *Phys. Rev. Lett.* **105**, 117003 (2010).
- [36] L. X. Yang, Y. Zhang, H. W. Ou, J. F. Zhao, D. W. Shen, B. Zhou, J. Wei, F. Chen, M. Xu, C. He, Y. Chen, Z. D. Wang, X. F. Wang, T. Wu, G. Wu, X. H. Chen, M. Arita, K. Shimada, M. Taniguchi, Z. Y. Lu, T. Xiang, and D. L. Feng, *Phys. Rev. Lett.* **102**, 107002 (2009).
- [37] T. Shimojima, W. Malaeb, A. Nakamura, T. Kondo, K. Kihou, C.-H. Lee, A. Iyo, H. Eisaki, S. Ishida, M. Nakajima, S. Uchida, K. Ohgushi, K. Ishizaka, and S. Shin, *Sci. Adv.* **3**, e1700466 (2017).
- [38] Y.-M. Xu, P. Richard, K. Nakayama, T. Kawahara, Y. Sekiba, T. Qian, M. Neupane, S. Souma, T. Sato, T. Takahashi, H.-Q. Luo, H.-H. Wen, G.-F. Chen, N.-L. Wang, Z. Wang, Z. Fang, X. Dai, and H. Ding, *Nat. Commun.* **2**, 392 (2011).

- [39] D. V. Evtushinsky, D. S. Inosov, V. B. Zabolotnyy, M. S. Viazovska, R. Khasanov, A. Amato, H-H. Klauss, H. Luetkens, Ch. Niedermayer, G. L. Sun, V. Hinkov, C. T. Lin, A. Varykhalov, A. Koitzsch, M. Knupfer, B. Büchner, A. A. Kordyuk, and S. V. Borisenko, *New J. Phys.* **11**, 055069 (2009).
- [40] D. V. Evtushinsky, D. S. Inosov, V. B. Zabolotnyy, A. Koitzsch, M. Knupfer, B. Büchner, M. S. Viazovska, G. L. Sun, V. Hinkov, A. V. Boris, C. T. Lin, B. Keimer, A. Varykhalov, A. A. Kordyuk, and S. V. Borisenko, *Phys. Rev. B* **79**, 054517 (2009).
- [41] T. Yokoya, T. Kiss, A. Chainani, S. Shin, M. Nohara, and H. Takagi, *Science* **294**, 2518 (2001).
- [42] K. Nakayama, T. Sato, P. Richard, Y.-M. Xu, Y. Sekiba, S. Souma, G. F. Chen, J. L. Luo, N. L. Wang, H. Ding, and T. Takahashi, *Europhys. Lett.* **85**, 67002 (2009).
- [43] K. Kuroki, S. Onari, R. Arita, H. Usui, Y. Tanaka, H. Kontani, and H. Aoki, *Phys. Rev. Lett.* **101**, 087004 (2008).
- [44] R. Yu, J.-X. Zhu, and Q. Si, *Phys. Rev. B* **89**, 024509 (2014).
- [45] T. Shimojima, F. Sakaguchi, K. Ishizaka, Y. Ishida, T. Kiss, M. Okawa, T. Togashi, C.-T. Chen, S. Watanabe, M. Arita, K. Shimada, H. Namatame, M. Taniguchi, K. Ohgushi, S. Kasahara, T. Terashima, T. Shibauchi, Y. Matsuda, A. Chainani, and S. Shin, *Science* **332**, 564 (2011).
- [46] M. Yi, A. Frano, D. H. Lu, Y. He, M. Wang, B. A. Frandsen, A. F. Kemper, R. Yu, Q. Si, L. Wang, M. He, F. Hardy, P. Schweiss, P. Adelman, T. Wolf, M. Hashimoto, S.-K. Mo, Z. Hussain, M. Le Tacon, A. E. Böhmer, D.-H. Lee, Z.-X. Shen, C. Meingast, and R. J. Birgeneau, *Phys. Rev. Lett.* **121**, 127001 (2018).
- [47] B. P. P. Mallett, P. Marsik, M. Yazdi-Rizi, Th. Wolf, A. E. Böhmer, F. Hardy, C. Meingast, D. Munzar, and C. Bernhard, *Phys. Rev. Lett.* **115**, 027003 (2015).
- [48] J. Hou, C.-W. Cho, J. Shen, P. M. Tam, I.-H. Kao, M. Hei, G. Lee, P. Adelman, and T. Wolf-RolfLort, *Physica C* **539**, 30 (2017).
- [49] K. Cho, M. Kończykowski, S. Teknowijoyo, M. A. Tanatar, J. Guss, P. B. Gartin, J. M. Wilde, A. Kreyssig, R. J. McQueeney, A. I. Goldman, V. Mishra, P. J. Hirschfeld, and R. Prozorov, *Nat. Commun.* **9**, 2796 (2018).
- [50] H. Eisaki, N. Kaneko, D. L. Feng, A. Damascelli, P. K. Mang, K. M. Shen, Z.-X. Shen, and M. Greven, *Phys. Rev. B* **69**, 064512 (2004).
- [51] M. R. Norman, M. Randeria, H. Ding, and J. C. Campuzano, *Phys. Rev. B* **57**, 11093(R) (1998).